N93-30857

DEVELOPMENTS IN IMPACT DAMAGE MODELING FOR LAMINATED COMPOSITE STRUCTURES[1]

Ernest F. Dost, William B. Avery, and Gary D. Swanson

The Boeing Company, Seattle, Washington

and

Kuen Y. Lin

University of Washington, Seattle, Washington

Introduction

Damage tolerance is the most critical technical issue for composite fuselage structures studied in ATCAS. The ATCAS program goals in damage tolerance include the characterization of impact damage, models for impact damage simulation, and understanding the behavior of notches and delaminations.

The characterization of potential impact damage states in fuselage is being accomplished through test. Configured structure will be impacted in different locations with a number of different impactor variables. The damage states will be assessed both nondestructively and destructively.

An approach for predicting the post-impact compressive behavior of laminated composites has been developed at Boeing over the past several years. Dr. K.Y. Lin and Dr. Z.Q. Chen at the University of Washington will be enhancing and generalizing this approach to account for the different potential damage states and failure modes found in the test program described above.

Tension damage tolerance is currently being addressed through a test program and analysis development by Dr. F.K. Chang at Stanford University. Future work with Dr. P.A. Lagace and Dr. M.J. Graves at Massachusetts Institute of Technology will address dynamic fracture including pressure effects.

Objectives

The objective of the work being presented is to understand both the impact damage resistance and residual strength of laminated composite fuselage structure. An understanding of the different damage mechanisms which occur during an impact event will (a) support the selection of materials and structural configurations used in different fuselage quadrants and (b) guide the development of analysis tools for predicting the residual strength of impacted laminates. Prediction of the damage state along with a knowledge of post-impact response to applied loads will allow for "engineered" stacking sequences and structural configurations; intelligent decisions on repair requirements will also result.
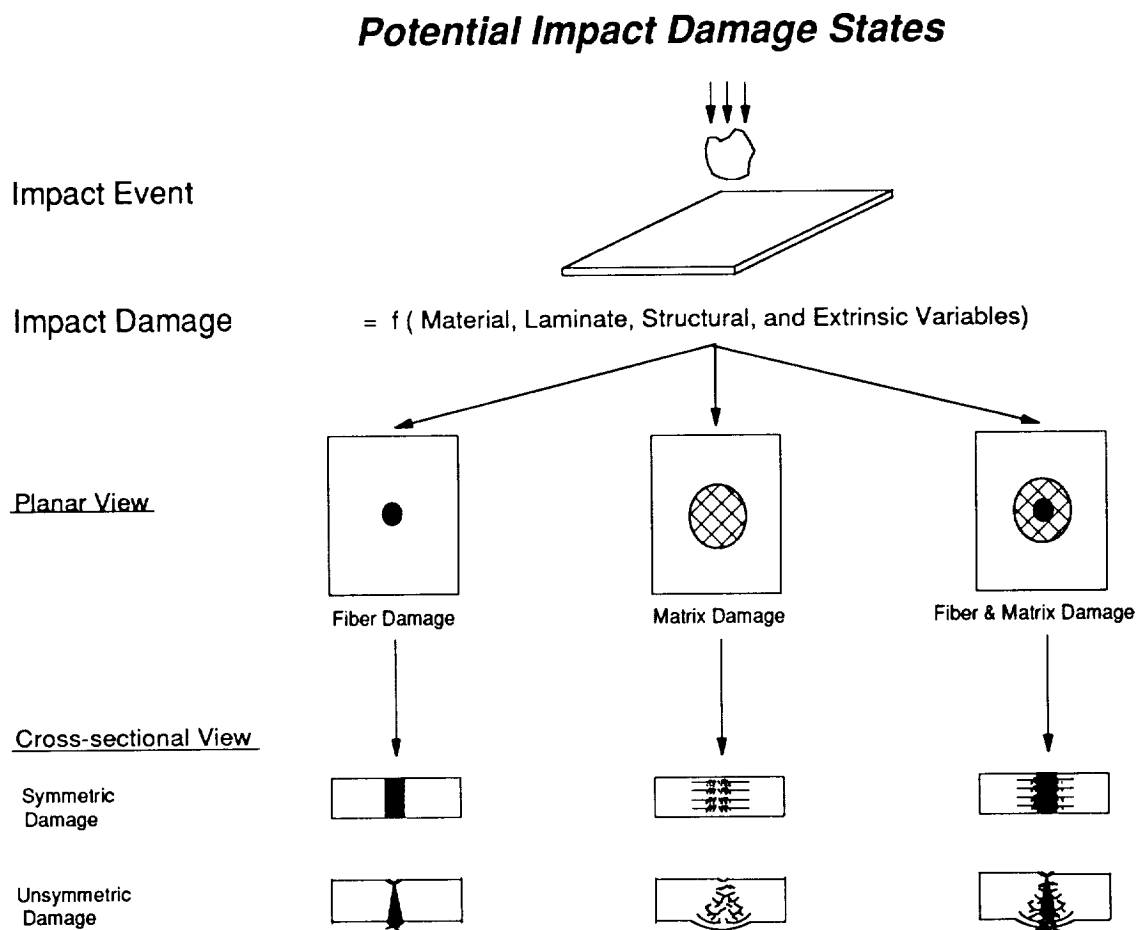
Potential Impact Damage States

A schematic diagram classifying characteristic damage states (CDS) that have been observed in flat laminates following low-velocity impact by spherical objects is shown. Planar and cross-sectional views of CDS are given in the figure. Three classes of CDS consisting of symmetric damage through the laminate cross section are shown in this figure. Damage size and type (fiber, matrix, or combined) depend on variables such as delamination resistance and impact energy. The most common damage observed in experiments with a stacking sequence used for material screening tests (i.e., $[45,0,-45,90,]_{nS}$) was matrix damage [1, 2].

Plate boundary conditions, laminate thickness, and material form are among the variables which may suppress delamination, causing damage dominated by fiber failure. Fiber damage, when present, tends to concentrate at the impact site. Matrix damage is also centered at the impact site, but tends to radiate away from this point to a size dependent on delamination resistance. The most general classification of symmetric damage involves both fiber and matrix failure.

Many factors can affect the CDS symmetry. Test observations have indicated thin laminates and heterogeneous stacking sequences tend to have unsymmetric CDS with damage concentrated opposite the impacted surface. Very thick laminates are also expected to have unsymmetric damage, but with damage concentrating closer to the impacted surface. Work by the current authors has indicated that delamination resistant materials have a stronger tendency for unsymmetric CDS than brittle materials tested with the same impact variables [3].

Potential Impact Damage States

Impact Event

Impact Damage = f (Material, Laminate, Structural, and Extrinsic Variables)

Planar View

Fiber Damage   Matrix Damage   Fiber & Matrix Damage

Cross-sectional View

Symmetric Damage

Unsymmetric Damage

Damage Modeling Applications

The panel shown below is a carbon fiber reinforced plastic (CFRP) wing gauge panel impacted on the stiffener cap. The impact damage located on this stiffener cap was nonvisible. An identical panel had been impacted on the stiffener attachment flange edge. Both panels had significant reductions in strength from their undamaged strength. Analytical tools developed to predict the post-impact response of CFRP structure must have enough generality to account for different failure modes which occur during impact. The approaches presented take into account both stress redistribution and changes in panel postbuckling response due to sublaminate buckling [1-3]. The prediction of post-impact response due to local fiber failures was presented by Cairns [4].

Impact Damage Discrete Modeling
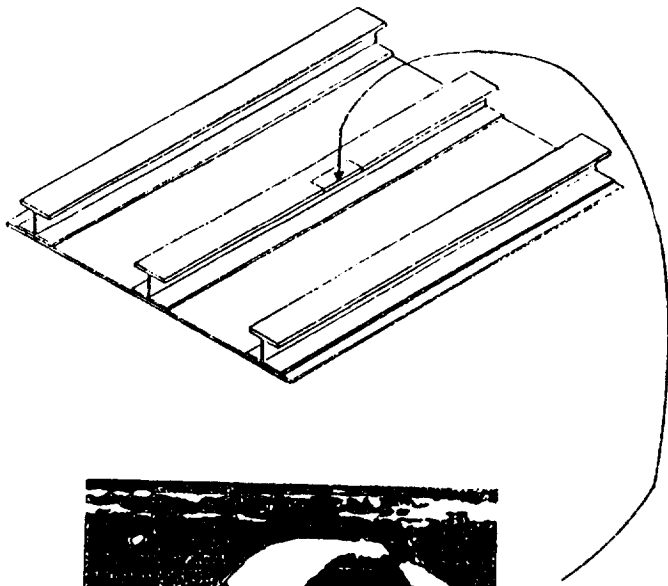
Wing Structure with Integral Stiffeners
Impacted on Free Flange
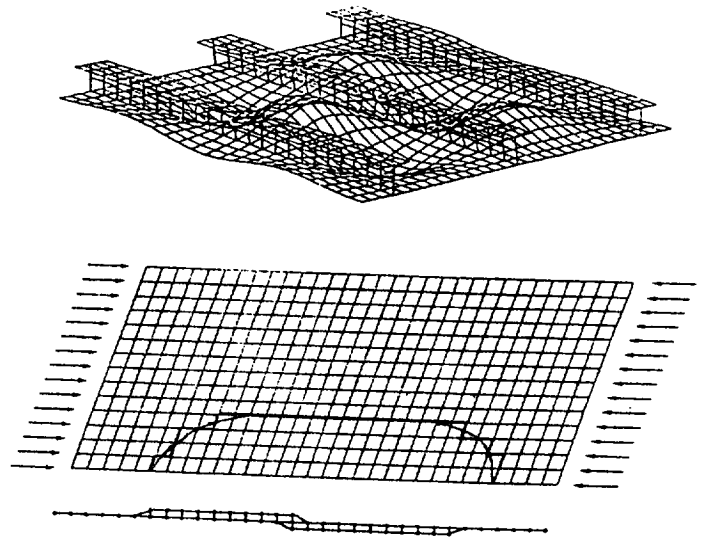
Global/Local Nonlinear Post-Buckling Analysis

Experimental Data Showing Post-impact Compression Performance as a Function of Laminate Stacking Sequence

Compression after impact (CAI) data are shown as a function of the drop weight impact energy (i.e., drop height x drop weight). Data scatter for each type of laminate layup was small compared to the total range of results. This indicated that laminate stacking sequence is critical to CAI. Note that all other material, laminate, structural, and extrinsic variables were held constant for the tests. The one exception was for the $[45_2,90_2,-45_2,0_2]_{2S}$ laminate which had 32 plies instead of 24 plies. Despite the additional thickness, this laminate did not have the highest CAI for a given impact energy, again indicating the importance of stacking sequence. These data illustrate that models to predict residual strength of impacted laminates must include stacking sequence dependent CDS details [3].

Experimental Data Showing Post-Impact Compression Performance as a Function of Laminate Stacking Sequence
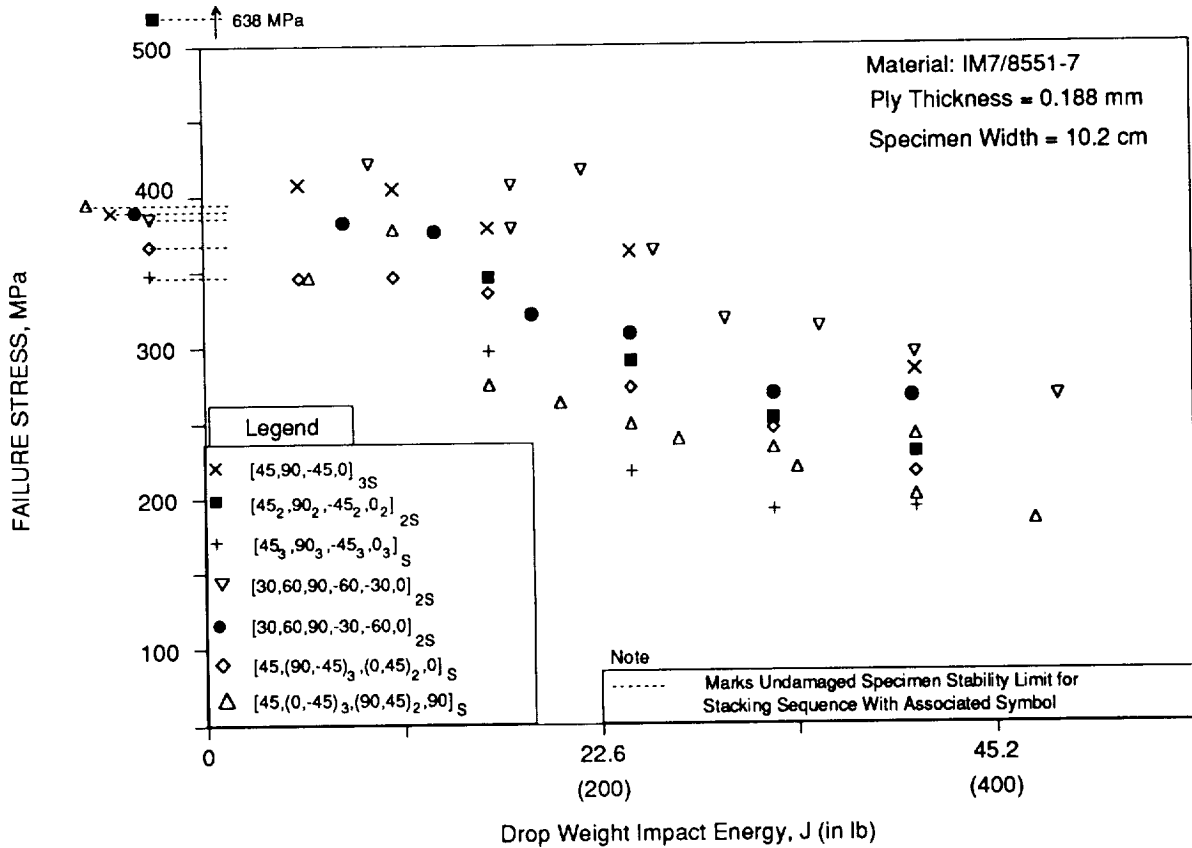
SUBLAMINATE STABILITY/REDUCED STIFFNESS CAI MODELING

The CDS for a set of impact variables used in material screening tests was described in earlier work [1,2,5]. These tests use a $[45,0,-45,90]_{nS}$ laminate stacking sequence. As discussed earlier, any fiber damage caused by impact tends to concentrate at the core of the CDS. A network of matrix cracks and delaminations comprise the remainder of the CDS. Delaminations at each ply interface are connected to those at neighboring ply interfaces by transverse matrix cracks. In a planar view, double-lobed delaminations formed at each interface. These delaminations are wedge shaped due to the $\pi/4$ difference in orientation of neighboring plies, breaking the CDS into octants. The ply orientation angles increase in $\pi/4$ increments from the impacted surface to the center. The stacking sequence and CDS is reflected at the center. Ply orientations decrease by $\pi/4$ with each ply from the center to the back side. This pattern causes a CDS with interconnected delaminations spiraling toward the center, reversing direction, and proceeding out toward the back side.

The CDS described above splits the laminate into separate sublaminates. These sublaminates are connected in a fashion similar to a spiral staircase, but are conceptualized as circular disks to simplify the analysis. The sublaminates near the outer surfaces vary in thickness from 2 to 5 plies. The next set of sublaminates are 4 plies in thickness with stacking sequence varying stepwise around the damage. This type of sublaminate can repeat several times, depending on the number of plies in the stacking sequence. Damage that occurs approaching both sides of the laminate midplane results in two discontinuous sublaminates and a symmetric core sublaminate that varies in thickness from 2 to 8 plies. The total number of sublaminates for a $[45,0,-45,90]_{nS}$ laminate stacking sequence is $(2n+1)$. This can be generalized for other repeating stacking sequences which increment by either decreasing or increasing ply angles if a sum of the difference between adjacent angles in the repeat element equals zero (i.e., $[\alpha,\beta,\phi,...,\theta]_{nS}$ where $\{\beta-\alpha\}+\{\phi-\beta\}+ ... +\{\alpha-\theta\} = 0.0$). Absolute values of each difference should also not exceed 90°.

The analysis method used for comparison with experiments is documented in [1,2]. In summary, five basic steps are followed in applying the method. First, the CDS is identified and simulated as a sublaminate with ply stacking sequence and thickness representing an average of those appearing in the real CDS. Second, a sublaminate stability analysis is performed using damage diameter as an independent variable characterizing the planar size of the CDS. This is done using a modification to the buckling analysis method described in [6]. The modification accounts for sublaminates with unsymmetric ply stacking sequences [1,2]. Third, effective reduced stiffness of the impact damage zone is calculated using results from sublaminate stability analysis. Fourth, the inplane stress concentration associated with the reduced stiffness is determined. Finite elements are used for this step in order to account for specimen width/damage size interactions. Finally, a maximum strain failure criteria is applied to predict CAI.

Note that steps 2 through 4 of the sublaminate stability analysis method should be modified for the most general CDS in which sublaminate parameters (e.g., diameter, thickness and stacking sequence) vary significantly through the laminate thickness. The more general model is currently being developed.

Experimental Determination of Sublaminate Buckling and Strain Distribution of Impacted Laminates

Sublaminate stability and subsequent load redistribution of compressively loaded impact damaged coupons are being examined experimentally. Moire interferometry was employed to measure both in-plane and out-of-plane displacements of impacted coupons as a function of load. A micro-Moire grid (600 lines/millimeter) used to measure inplane displacements was applied to the tool side while the other side used shadow Moire (60 lines/cm) to measure out-of-plane displacements. A typical Moire fringe pattern displaying out-of-plane displacements for a $[45,0,-45,90]_{3S}$ specimen with a damage diameter of 1.28" is shown. The in-plane u-displacements are shown next to it. By examination of the in-plane displacement contours, one can discern that an inplane strain concentration occurs near the damage area.
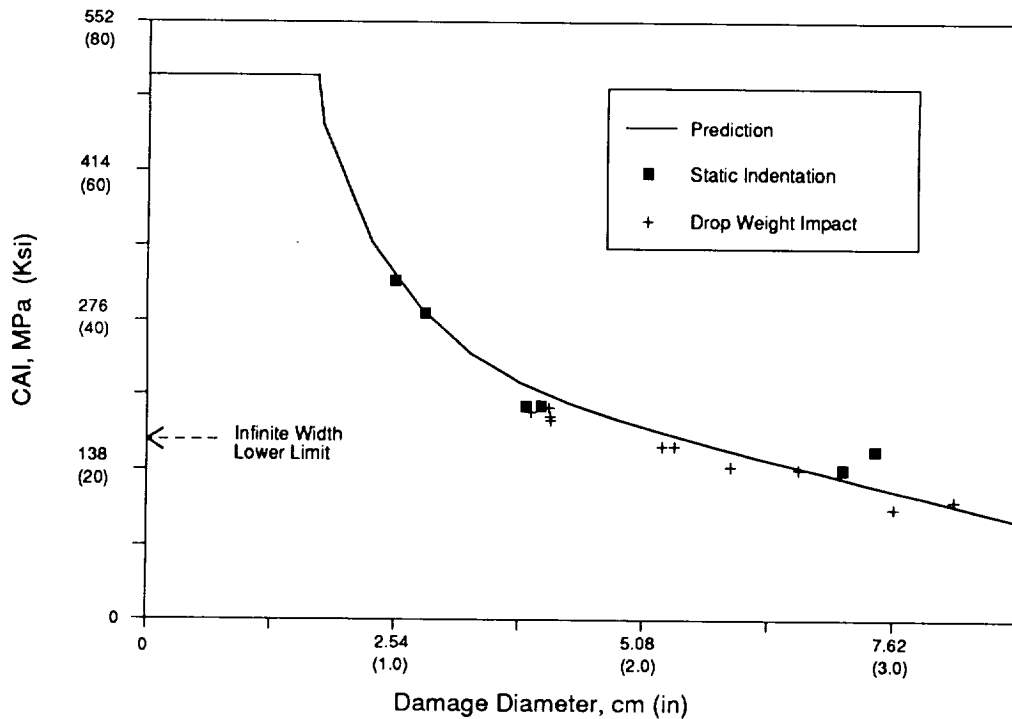

Out-of-Plane Displacement Contours

In-Plane Displacement Contours

726
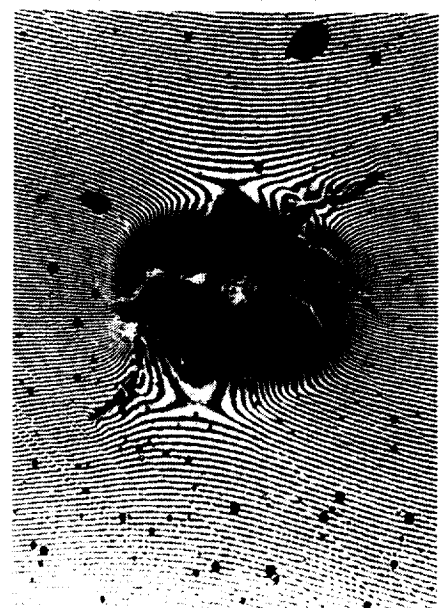
Sublaminate Stability/Reduced Stiffness and
Experimental Results for AS6/3501-6, $(45,0,-45,90)_{5S}$

This figure shows good comparisons between predictions and experimental results using a graphite/epoxy material (AS6/3501-6). The undamaged compressive strength was measured as 501 MPa (72.7 Ksi). Damage was created by both static indentation and drop weight impact. Finite specimen width becomes important as damage diameters increase. As shown, the model accurately predicted CAI throughout the range studied. The CAI lower limit for infinitely wide coupons would correspond to the maximum stress concentration of three for a quasi-isotropic laminate (i.e., 167 MPa).

Sublaminate Stability/Reduced Stiffness Predictions and Experimental Results for AS6/3501-6, $(45,0,-45,90)_{5S}$

Legend:
- —— Prediction
- ■ Static Indentation
- + Drop Weight Impact

Y-axis: CAI, MPa (Ksi)
X-axis: Damage Diameter, cm (in)

Infinite Width Lower Limit

Impact Damage Behavior of Curved Laminates

The influence of laminate curvature on damage resistance and post-impact compression strength was investigated for a "brittle" material system. The stacking sequence was $(45/90/-45/0)_{3S}$ and the nominal laminate thickness was 0.38 cm. The dimensions of the flat panels were 10.2x15.2 centimeters with the 15.2 cm direction parallel to the 0 degree direction of the laminate. The curved laminates were cylindrical in shape with a radius of curvature of 22.9 cm and dimensions of 10.2x15.2 centimeters. The impact procedure was performed by placing the coupons in a support fixture that approximates simply supported boundary conditions. Coupons were held with clamps on both sides to prevent rebound during impact. A special fixture was fabricated for the curved panels such that the curvature of the fixture matched the curvature of the test coupons. Impacting was performed using an instrumented impact tower. During the post-impact compression tests, the coupons were mounted in a side-supported fixture developed by The Boeing Company for compression residual strength tests. A special modification of the fixture was fabricated to enable compression testing of the curved panels.

Damage area as a function of impact energy is presented in the first figure below. The flat panels exhibited a maximum damage diameter of approximately 4 cm, whereas the curved laminates exhibited damage diameters of up to 8.5 cm before significant interaction with boundaries occurred. Recalling that the total width of a coupon is 10.2 cm indicates that significant area of the coupon was damaged. The massive increase in damage area in the curved coupons is believed due to the curvature induced increase in laminate stiffness, which results in higher impact and shear loads. Further analysis of curvature effects is continuing.

Post-impact compression strength as a function of damage area is presented in the second figure. The curved panels exhibited higher CAI strength for a given damage area. This is assumed due to the increase in stability imparted by coupon curvature..

Damage Resistance: Flat versus Curved Panel (45,90,-45,0)$_{3S}$
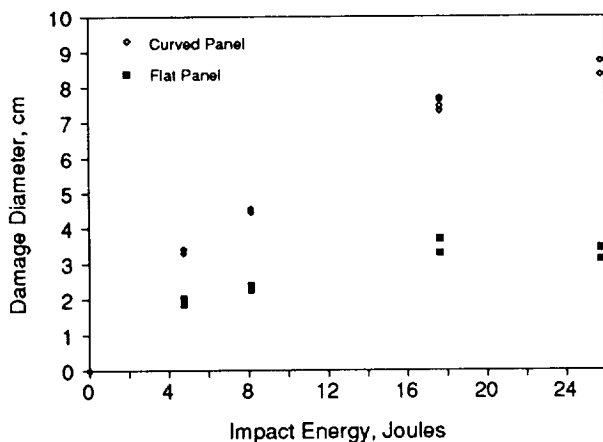
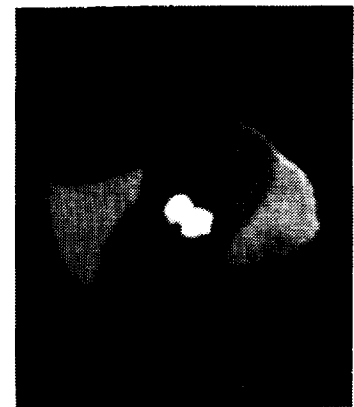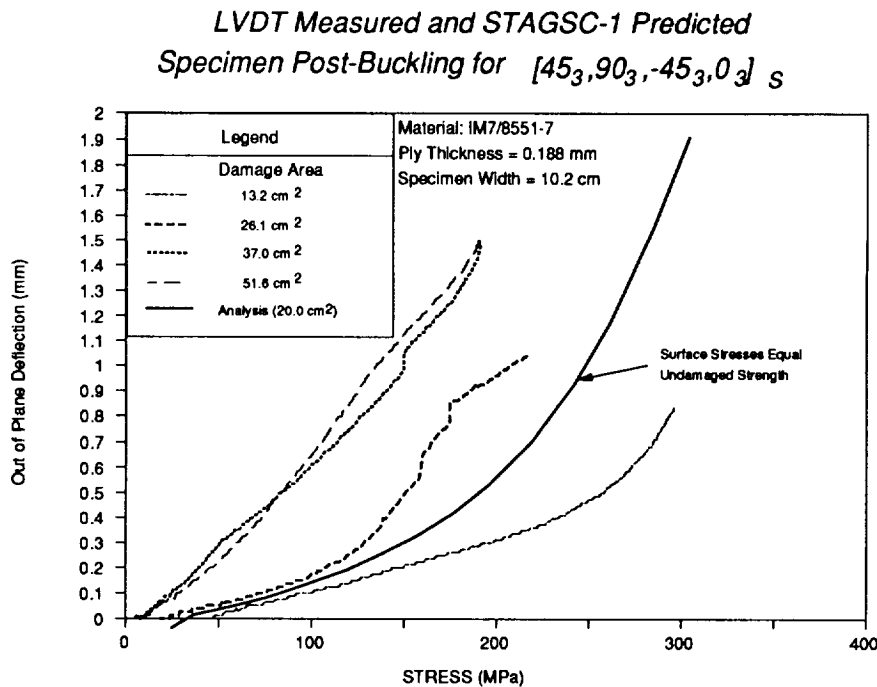*Residual Strength: Flat versus Curved Panel (45,90,-45,0)$_{3S}$*

728
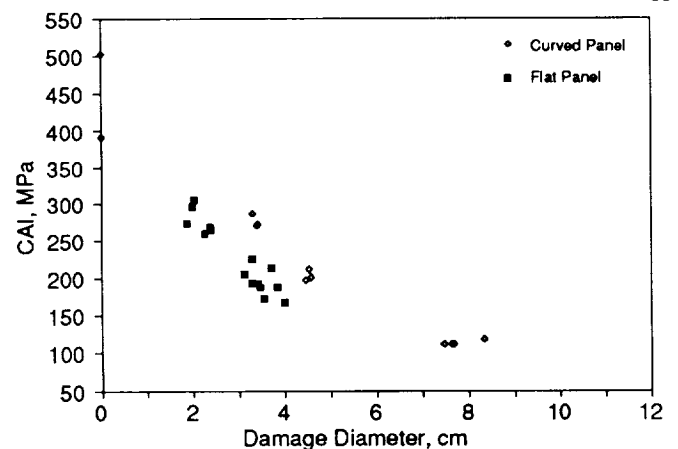
LVDT Measured and STAGSC-1 Predicted
Specimen Post-Buckling for $(45_3,90_3,-45_3,0_3)_S$

The large delaminations visible in the ultrasonic c-scan occur in the back half of the $[45_3,90_3,-45_3,0_3]_S$ laminate, effectively breaking it into two sublaminates. The sublaminate located toward the back side has octants containing 0, 3, 6 and 9 plies while the thicker, base sublaminate has octants containing 24, 21, 19, and 15 plies, respectively.

Despite a limited number of test results, post impact failure data trends were found to vary significantly from sublaminate stability/reduced stiffness prediction for this laminate. The most striking difference occurred for large damage areas where a finite width effect was not evident in the data [3].

A STAGSC-1 [7] geometrically nonlinear finite element (FE) analysis was performed on a discrete sublaminate model using damage details described above to better understand the observed behavior. The FE results are plotted together with experimental measurements of out-of-plane displacement versus load. The analysis demonstrated that specimen stability was affected by sublaminate stability. Outward buckling in the +Z direction of the sublaminate forced overall coupon instability in this direction. The change in specimen stability resulting from sublaminate buckling exhibits trends similar to those observed in postbuckling analysis with increasing applied imperfections.

Out-of-plane specimen displacements were measured with a linear variable displacement transducer (LVDT). It can be seen that the amount of "imperfection" imparted to the specimen increases with damage size. The predicted displacements for 20.0 cm^2 damage area fall between experimental data curves for 13.2 and 26.1 cm^2 damage areas in the figure below. Note that the out-of-plane displacement corresponding to a surface stress of 478 MPa (undamaged compressive strength) in the model was 0.95 mm. This also compares well with the experimental data for 13.2 and 26.1 cm^2.

LVDT Measured and STAGSC-1 Predicted
Specimen Post-Buckling for $[45_3,90_3,-45_3,0_3]_S$

Legend

Damage Area
————	13.2 cm^2
– – – –	26.1 cm^2
·········	37.0 cm^2
— —	51.6 cm^2
———	Analysis (20.0 cm2)

Material: IM7/8551-7
Ply Thickness = 0.188 mm
Specimen Width = 10.2 cm

Surface Stresses Equal
Undamaged Strength

Out of Plane Deflection (mm)

STRESS (MPa)

Pulse-Echo C-Scan

Impact Energy = 40.7 Joules

Effect of Damage on Stiffness and Stability

The previous chart demonstrated that impact damage can significantly alter panel stability. Analytical studies on the effect of hypothetical damage on coupon stability were performed to examine this. Two types of simulated damage were used in these studies, both having an axial stiffness reduction of 50%. The symmetric damage was simulated with a 50% reduction in axial moduli, while unsymmetric damage was simulated with 1/2 the laminate stacking sequence and an offset. Analyses were run with damage simulations in the middle and on the edge of 24" by 12" rectangular plates. Damage size was varied from 2" x 2" to 5" x 5".

Center damage was found to lower initial buckling load for small damage sizes. As damage size increased the postbuckling mode shape changed from two halfwaves to a single halfwave. A stiffer postbuckling response was associated with this switch in mode shape. Plates with unsymmetric damage had a lower postbuckling stiffness than those with symmetric damage. Both symmetric and unsymmetric simulated damage on the edge of a plate were found not to change postbuckling mode shape. Postbuckling stiffness was found to decrease with increasing damage size. The difference in postbuckling stiffness between symmetric and unsymmetric damage tended to increase with increasing damage size, with unsymmetric damage having a lower stiffness.

The effect of hypothetical damage on stiffened panel stability was examined using analytical studies similar to those described previously. The simulated damage used in these studies was symmetric and had an axial stiffness reduction of 90% in a 1"x1" core region surrounded by 4"x2" 50% reduced stiffness zone. Analyses were run with the damage simulation at the edge of the stiffener attaching flange for both hat and blade stiffened panels. There was negligible change in postbuckling response of these panels for the described damage. Note: This was not nessesarily the worst case scenario, but a demonstration of the concept. Other damage states and locations may have more effect on panel response.

Effect of Damage on Stiffness and Stability

730
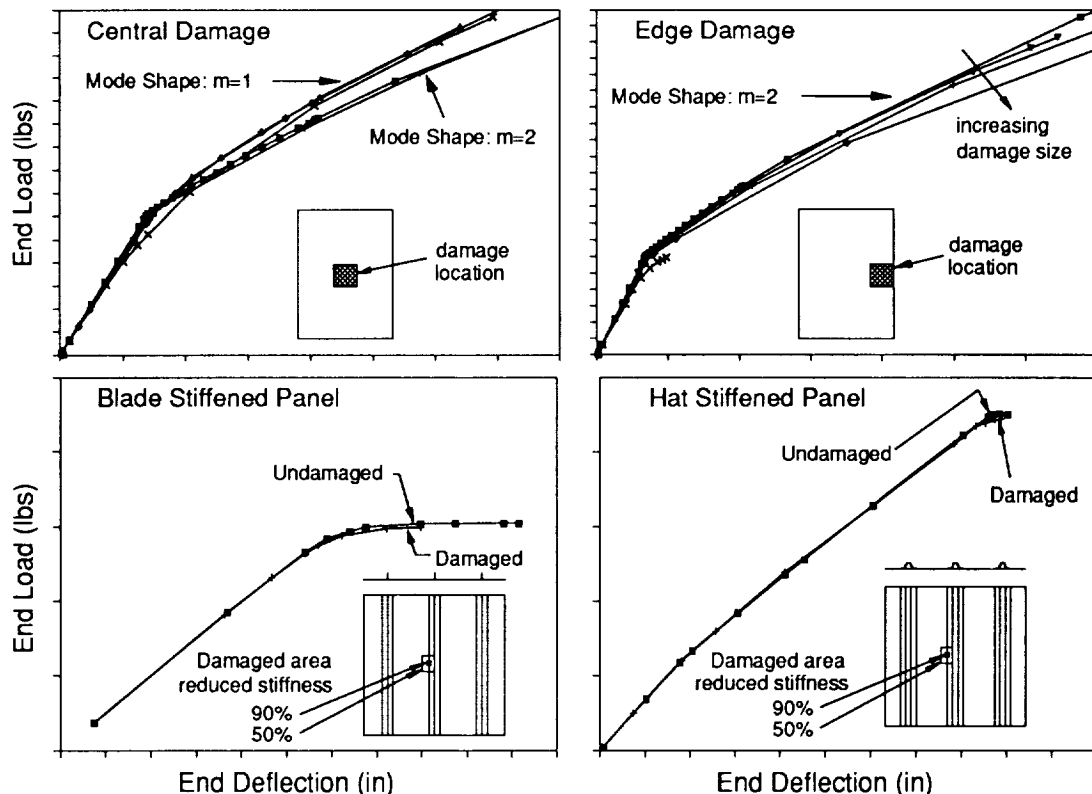
Impact Designed Experiment Involving Multiple Variables

A statistically based designed experiment is being used to study impact damage resistance of fuselage structure. A total of 16 variables are being investigated to determine their relative importance to different potential failure modes. Interactions between variables are believed to be important; therefore, the approach of changing one variable at a time is inadequate. A fully crossed experiment would yield information on all main effects and all interactions, but would require 65536 tests (not including replication) when studying 16 variables. A fractional factorial design provides an understanding of all main effects and significant insight to interactions with only 32 tests [8].

A significant number of variables listed below relate to the impactor. Past impact studies have been performed using aircraft assembly/maintainance tools and other inservice threats for evaluation impact damage. The 1.0" diameter hemispherical impactor was found to produce the same results as the majority of possible threats. "Brittle" materials of the day tended to absorb impact energy through the creation of delaminations and transverse cracks which would dominate compression after impact strength (CAI). The large delaminations effectively decreased the local flexural stiffness, reducing contact pressures, and hence local fiber failures. Composite materials development concentrated on increasing CAI by reducing damage size. Smaller damage sizes lead to higher contact pressures and more fiber failure; thus impactor variables such as shape, size, and stiffness may be accentuated.

Results from this experimental study will guide material and structural configuration decisions for aircraft fuselage structures. It will also provide guidance in the development of analysis tools for predicting post-impact performance of composite structures.
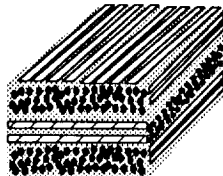
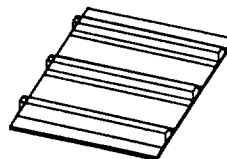## Impact Designed Experiment Involving Multiple Variables

Material Variables	Laminate Variables	Structural Variables	Extrinsic Variables
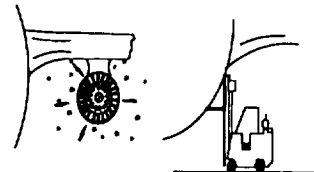
Fiber	Stiffener Layup	Stiffener Type	Impact Mass
AS4	Hard	Blade	0.5 lbm.
IM7	Soft	Hat	12.0 lbm.
Resin	Skin Layup		Impact Energy (Skin/Stiffener)
938 (3501-6)	Hard	Stiffener Spacing	80 in lb / 200 in lb
977-2	Soft	7 in.	1200 in lb / 2000 in lb
Fiber Volume	Thickness	12 in.	Impact Temperature
0.480	Thick (Approx. 0.2 in.)	Stiffener Adhesive	70° F
0.565	Thin (Approx. 0.1 in.)	Layer	180° F
Material Form		With	Impactor Diameter
Tape		Without	0.25 in.
Tow			1.0 in.
			Impactor Tup Shape
			Flat
			Spherical
			Impactor Stiffness
			0.5 Msi
			30 Msi

Fuselage Locations Represented by Test Panels

The panel configurations and materials chosen for the impact damage resistance designed experiment are representative of a variety of locations around the fuselage. The fuselage crown is tension dominated structure and hence a stiffener spacing of 12.0 inches and thin skin gages can be used. The fuselage keel on the other hand is compression dominated and requires a closer stiffener spacing and thicker gages. Matrix material toughness may be required for the keel when considering high levels of impact energy resulting impact from runway debris. The crown, however has hail impact as a design criteria and may not require costly toughened materials to resist damage. The panels built for this experiment have combinations of the variables listed above covering a range of locations on the fuselage.

Fuselage Locations Represented by Test Panels
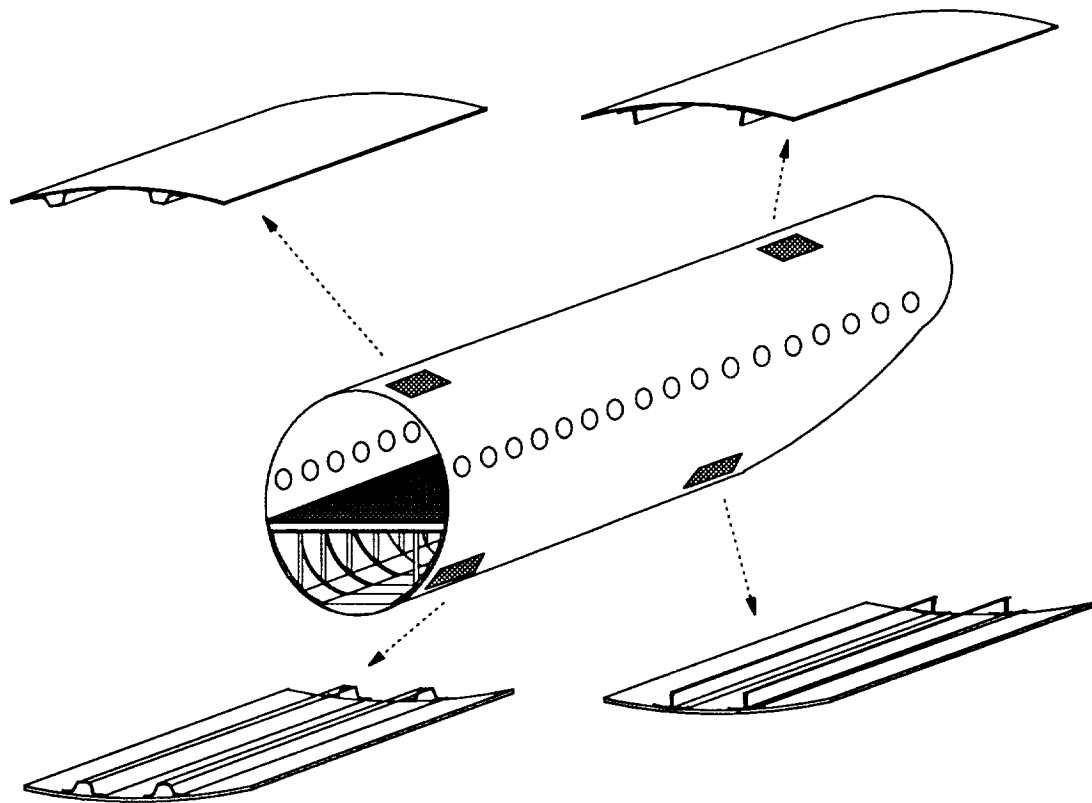
## Integrated Approach to Manufacturing Demonstration and Structural Performance

Design, manufacturing , and material selection for low-cost composite fuselage are made by the Boeing ATCAS Design Build Team. The selection criteria is based on a potential for low cost and weight in the fully assembled structure. The panels fabricated for ATCAS serve multi-functions devised to develop and validate composite manufacturing and structures technologies. Manufacturing trials and test articles for performance evaluation are coupled. This results in an efficient use of contract funds and allows test evaluation of process anomalies characteristic of panels fabricated with design details. To date, panel fabrication in ATCAS has evaluated (1) drape forming and tooling concepts for a low cost stiffener fabrication process, (2) advanced fiber placement for skin panels that include ply drop-offs characteristic of fuselage design, (3) process modifications for eight material types identified as candidates for fuselage structures. The 110 in. stiffened panels fabricated will be machined into specimens and test elements for assembly trials, impact damage resistance evaluation, damage tolerance tests, and stiffness/stability measurements.

Integrated Approach to Manufacturing Demonstration and Structural Performance

Representative panels fabricated to support
- Low cost process development
- Tests of fuselage performance issues
- Material and design selections

65C35529-4
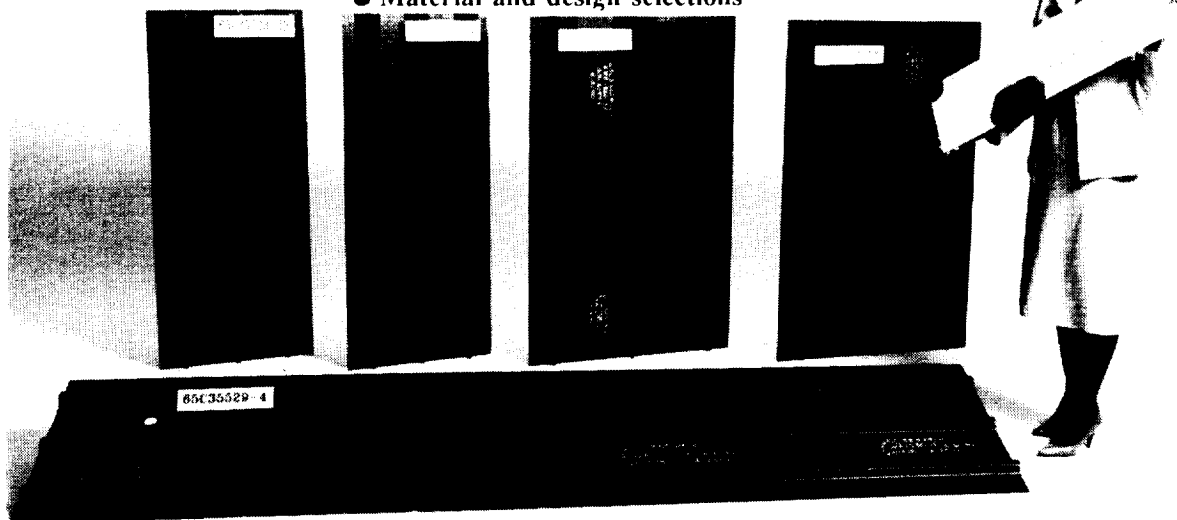
NASA/BOEING
ATCAS

Critical Impact Locations

All 32 impact damage resistance panels will be impacted at the structural locations shown below. These are thought to represent those most critical for stiffened panels of this sort. All impacts will be instrumented to determine force/time relations. Each impact site will be nondestructively inspected to determine the maximum extent of damage created. Final impact locations will be based on extent and location of previous impact damage sites.

The impact damage states will be characterized both in terms of lateral extent and through-the-thickness distribution of matrix and fiber damage. The impact sites will be inspected using time-of-flight pulse-echo ultrasonics to map out delamination depth and extent. Resin burnoff will be used to map out fiber failures which exist. Coupons will be machined and compressively tested to failure. The variables will then be ranked versus the different failure modes and residual strength to determine which variables and variable interactions are most significant to each failure mode.
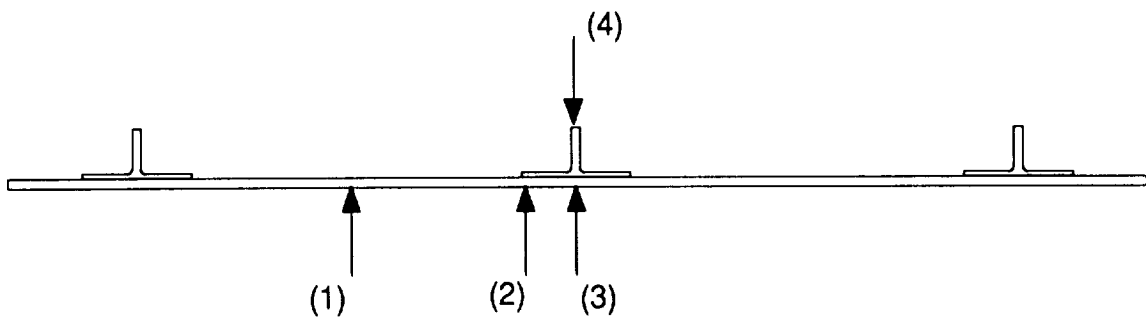
CRITICAL IMPACT LOCATIONS
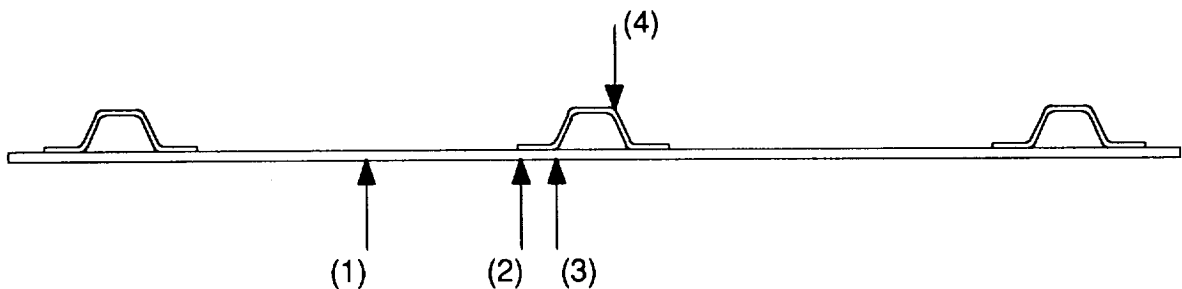
(1) Skin Midbay
(2) Edge of Stiffener Attachment Flange
(3) Base of Stiffener Web
(4) Top of Stiffener

Impact Damage Resistance/Residual Strength
# of Sandwich Structure for Aircraft Fuselage

Impact damage resistance/residual strength of sandwich panels will be investigated experimentally to define impact damage related structural requirements for aircraft fuselage. Past investigations of low velocity impact on sandwich structure have been performed on panels with thin gauge face sheets and low density cores to support secondary structure applications. These typically have studied skin gauges less than 0.05 inch and core densities between 3 and 6 lb/ft^3 [9,10]. Impact damage resistance/residual strength studies will be performed on laminates with facesheets ranging from 0.15 to 0.3 inches and core densities from 6 to 18 lb/ft^3.

The response of tapered structure to impact damage will be studied. The 10.0 inch long tapered region of the stiffened panel designed experiment will be fabricated into sandwich panels with a 3/4 inch core, representative of the aircraft keel. Facesheet delamination/transverse cracking, fiber damage, and core shear/crushing failures will be the measured responses.

Impact Damage Resistance/Residual Strength
of Sandwich Structure for Aircraft Fuselage

Constant Gauge

Tapered

Variables
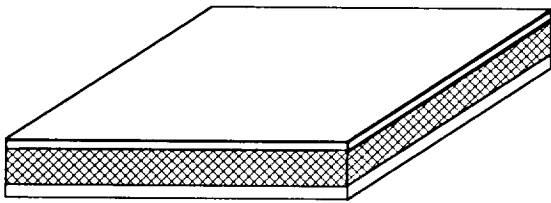
Core Type: Foam vs. Honeycomb

Core Density: 6 - 18 lbs/ft^3

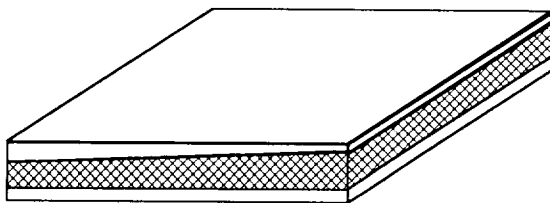Core Thickness: 0.25 - 0.75 inches

Face Sheet Thickness: 0.1 - 0.3 in.

Fiber Type: AS4 vs. IM7

Matrix Type: 3501-6 vs. 8551-7

Impactor Shape: Flat vs. Spherical

Impactor Diameter: 0.25 - 1.0 in.

Laminate Layup: Hard vs. Soft

Fiber Type: AS4 vs. IM7

Matrix Type: 938 vs. 977-2

Fiber Volume: 0.480 vs. 0.565

Material Form: Tow vs. Tape

Summary

Models to predict residual strength of impacted laminates must include stacking sequence dependent details of the damage state.

CAI for laminates with symmetric size distributions of matrix damage through the thickness was predicted with a sublaminate stability/stress redistribution analysis method.

Post-impact performance for laminates with unsymmetric size distributions of matrix damage through the thickness was best termed a change in specimen stability.

Variables most crucial to fuselage impact damage resistance will be identified.

References

1.) Dost, E.F., Ilcewicz, L.B., and Gosse, J.H., "Sublaminate Stability Based Modeling of Impact Damaged Composite Laminates," in Proc. of 3rd Tech. Conf. of American Soc. for Composites, Technomic Publ. Co., 1988, pp. 354-363.

2.) **Ilcewicz, L.B., Dost, E.F., and Coggeshall, R.L., "A Model for Compression After Impact Strength Evaluation," in Proc. of 21st Inter. SAMPE Tech. Conf., Soc. for Advanc. of Material and Process Eng., 1989, pp. 130-140.**

3.) **Dost, E.F., Ilcewicz, L.B., and Avery, W.B., "The Effects of Stacking Sequence On Impact Damage Resistance and Residual Strength for Quasi-Isotropic Laminate," in Composite Materials: Fatigue and Fracture, ASTM STP 1110, 1991.**

4.) Cairns, D.S. and Lagace P.A., "Residual Tensile Strength of Graphite/Epoxy and Kevlar/Epoxy Laminates with Impact Damage," Massachusetts Institute of Technology, TELAC Report 88-3, 1988.

5.) Gosse, J.H., and Mori, P.B.Y., "Impact Damage Characterization of Graphite/Epoxy Laminates," in Proc. of 3rd Tech. Conf. of American Soc. for Composites, Technomic Publ. Co., 1988, pp. 344-353.

6.) Shivakumar, K.N., and Whitcomb, J.D., "Buckling of a Sublaminate in a Quasi-Isotropic Composite Laminate," J. Composite Materials, Vol. 19, 1985, pp 2-18.

7.) Almroth, B.O., Brogan, F.A., and Stanley, G.M., Structural Analysis of General Shells, Vol. 2 User Instructions for STAGS-C1, Lockheed Palo Alto Research Laboratory, Palo Alto, CA, Jan. 1983.

8.) Wheeler, D.J., Understanding Industrial Experimentation, Statistical Process Controls, Inc., Knoxville, Tenn. 37919.

9.) Rhodes, M.D., "Low Velocity Impact on Composite Sandwich Structures," Presented at the Second Air Force conference on Fibrous Composites in Flight Vehicle Design, Dayton, Ohio, May 22-24, 1974.

10.) Bernard, M.L., "Impact Resistance and Damage Tolerance of Composite Sandwich Plates," Massachusetts Institute of Technology, TELAC Report 87-11, 1987.

*References in bold were published while under Contract NAS1-18889.